別紙５

研究成果の刊行に関する一覧表レイアウト（参考）

２００６年以降

書籍

著者氏名	論文タイトル名	書籍全体の編集者名	書　籍　名	出版社名	出版地	出版年	ページ

雑誌

発表者氏名	論文タイトル名	発表誌名	巻号	ページ	出版年
Y. Haba, C. Kojima, A. Harada, K. Kono	Comparison of thermosensitive properties between poly(amidoamine) dendrimers having peripheral N-isopropylamide groups and linear polymers with the same groups	**Angew. Chem. Int. Ed.**	**46**	234-237	2007
Y. Haba, C. Kojima, A. Harada, K. Kono	Control of temperature-sensitive properties of poly(amidoamine) dendrimers using peripheral modification with various alkylamide groups	**Macromolecules**	**39**	7451-7453	2006
N. Sakaguchi, C. Kojima, A. Harada, K. Koiwai, K. Shimizu, N. Emi, K. Kono	Enhancement of transfection activity of lipoplexes by complexation with transferrin-bearing fusogenic polymer-modified liposomes	**Int. J. Pharmaceutics**	**325**	186-190	2006

別紙５

研究成果の刊行に関する一覧表

雑誌

発表者氏名	論文タイトル名	発表誌名	巻	ページ	出版年
Doshi M, Koyanagi M, Nakahara M, Saeki K, Saeki K, Yuo A	Identification of human neutrophils during experimentally induced inflammation in mice transplanted with human umbilical cord blood CD34-positive cells	Int J Hematol	84	231-237	2006

別紙５

研究成果の刊行に関する一覧表レイアウト（参考）

書籍

著者氏名	論文タイトル名	書籍全体の編集者名	書　籍　名	出版社名	出版地	出版年	ページ

雑誌

発表者氏名	論文タイトル名	発表誌名	巻号	ページ	出版年
Terui Y, Sakurai T, Mishima Y, Mishima Y, Sugimura N, Sasaoka C, Kojima K, Yokoyama M, Mizunuma N, Takahashi S, Ito Y, Hatake K.	Blockade of bulky lymphoma-associated CD55 expression by RNA interference overcomes resistance to CDC with rituximab.	Cancer Science.	97	72-79	2006
Mishima Y, Terui Y, Sugimura N, Matsumoto-Mishima Y, Rokudai A, Kuniyoshi R, Hatake K.	Continuous treatment of bestatin induces anti-angiogenic property in endothelial cells.	Cancer Sci.	98	in press	2007
Utsubo-Kuniyoshi R, Terui Y, Mishima Y, Rokudai A, Mishima Y, Sugimura N, Kojima K, Sonoda Y, Kasahara T, Hatake K.	MEK-ERK is involved in SUMO-1 foci formation on apoptosis.	Cancer Sci.	in perss		

別紙５

研究成果の刊行に関する一覧表レイアウト（参考）

書籍

著者氏名	論文タイトル名	書籍全体の編集者名	書　籍　名	出版社名	出版地	出版年	ページ
なし							

雑誌

発表者氏名	論文タイトル名	発表誌名	巻号	ページ	出版年
Sanae Uchida, 他6名	Amino acids C-terminal to the 14-3-3 binding motif in CDC25B affects the efficiency of 14-3-3 binding.	Journal of Biochemistry	139（4）	761-769	2006
Megumi Matsumoto, 他11名	Purturbed Gap-filling Synthesis in Nucleotide Excision Repair Causes Histone H2AX Phosphorylation in Human Quiescent Cells.	Journal of Cell Science	120（6）	In press	2007

Oncogene (2006), 1–10

www.nature.com/onc

ORIGINAL ARTICLE

HIV-1 Vpr induces ATM-dependent cellular signal with enhanced homologous recombination

C Nakai-Murakami[1], M Shimura[1], M Kinomoto[2], Y Takizawa[3], K Tokunaga[2], T Taguchi[1], S Hoshino[1], K Miyagawa[4], T Sata[2], H Kurumizaka[3], A Yuo[1] and Y Ishizaka[1]

[1]Departments of Intractable Diseases and Hematology, International Medical Center of Japan, Shinjuku-ku, Tokyo, Japan; [2]Department of Pathology, National Institute of Infectious Diseases, Shinjuku-ku, Tokyo, Japan; [3]Waseda University School of Science and Engineering, Shinjuku-ku, Tokyo, Japan and [4]Section of Radiation Biology, Graduate School of Medicine, The University of Tokyo, Bunkyo-ku, Tokyo, Japan

An ATM-dependent cellular signal, a DNA-damage response, has been shown to be involved during infection of human immunodeficiency virus type-1 (HIV-1), and a high incidence of malignant tumor development has been observed in HIV-1-positive patients. Vpr, an accessory gene product of HIV-1, delays the progression of the cell cycle at the G2/M phase, and ATR–Chk1-Wee-1, another DNA-damage signal, is a proposed cellular pathway responsible for the Vpr-induced cell cycle arrest. In this study, we present evidence that Vpr also activates ATM, and induces expression of γ-H2AX and phosphorylation of Chk2. Strikingly, Vpr was found to stimulate the focus formation of Rad51 and BRCA1, which are involved in repair of DNA double-strand breaks (DSBs) by homologous recombination (HR), and biochemical analysis revealed that Vpr dissociates the interaction of p53 and Rad51 in the chromatin fraction, as observed under irradiation-induced DSBs. Vpr was consistently found to increase the rate of HR in the locus of I-*SceI*, a rare cutting-enzyme site that had been introduced into the genome. An increase of the HR rate enhanced by Vpr was attenuated by an ATM inhibitor, KU55933, suggesting that Vpr-induced DSBs activate ATM-dependent cellular signal that enhances the intracellular recombination potential. In context with a recent report that KU55933 attenuated the integration of HIV-1 into host genomes, we discuss the possible role of Vpr-induced DSBs in viral integration and also in HIV-1 associated malignancy.
Oncogene advance online publication, 18 September 2006; doi:10.1038/sj.onc.1209831

Keywords: HIV-1; Vpr; DNA double-strand breaks; homologous recombination; Non-AIDS defining malignancies

Introduction

The induction of a cellular response similar to DNA-damage-sensing signals has been shown during human immunodeficiency virus type-1 (HIV-1) infection (Daniel *et al.*, 1999, 2003, 2004, 2005; Lau *et al.*, 2004). The synthesis of linear HIV-1 DNA in the cytoplasm by reverse transcription and the integration process of HIV-1 DNA into the host genome are thought to be possible triggers for the DNA-damage signals (Lau *et al.*, 2004, 2005). When chromosomal DNA is damaged (DSB; DNA double-strand break), two kinds of kinases (ATM and ATR) are initially activated to exert checkpoint control on cell cycle (Abraham, 2001). When caffeine, which is known to inhibit both ATR and ATM, is administered in conjugation with the viral infection, the integration of viral DNA into the host genome is impaired (Daniel *et al.*, 2005). Additionally, data showing that the recently developed ATM inhibitor KU55933 decreased the copy number of the integrated HIV-1 DNAs strongly suggest that an ATM-dependent signal has a key role in viral transduction (Lau *et al.*, 2005). In addition to the mechanism of viral infection, HIV-1-induced DSBs or their signals have an impact on the approaching AIDS pathogenesis, especially for cancer development. A high incidence of malignant tumors has been reported in AIDS patients (Mayer *et al.*, 1995; Biggar *et al.*, 1996; Straus, 2001), and recent observations have indicated that tumor development is observed even in HIV-1-positive patients who do not show any immunocompromised manifestations (Knowles, 2003). These data suggest that HIV-1 infection is by itself oncogenic (Laurence and Astrin, 1991), but the viral protein responsible for ATM activation during HIV-1 infection has not been well characterized.

Vpr, an accessory gene product of HIV-1, impairs the progression of the cell cycle at G2/M phase (He *et al.*, 1995; Goh *et al.*, 1998). Vpr is thought to inactivate Cdc2, which is a component of maturation-promoting factor, by phosphorylating tyrosine 15 (Bukrinsky and Adzhubei, 1999; Elder *et al.*, 2002). Recent studies have shown that Vpr-induced G2 arrest is attenuated by the introduction of *wee-1* siRNA or deletion of the *wee-1*

Correspondence: Dr Y Ishizaka, Department of Intractable Diseases, International Medical Center of Japan, 1-21-1 Toyama, Shinjuku-ku, Tokyo 162-8655, Japan.
E-mail: zakay@ri.imcj.go.jp
Received 22 August 2005; revised 12 May 2006; accepted 12 June 2006

gene (Yuan *et al.*, 2004). Together with data on a dominant-negative mutant of ATR and its siRNA, ATR–Chk2–Wee-1 as a summarized signal pathway was postulated to be responsible for the Vpr-induced G2 arrest (Roshal *et al.*, 2003; Yuan *et al.*, 2004; Zimmerman *et al.*, 2004). As an earlier study demonstrated that ATM was not important for Vpr-induced G2 arrest (Bartz *et al.*, 1996), there have been no reports that describe the activation of ATM under Vpr expression. To investigate the Vpr-induced cell cycle abnormalities, we established a MIT-23 cell line, in which Vpr expression is tightly regulated by a tetracycline promoter (Shimura *et al.*, 1999b). We found that the continuous expression of Vpr induced the formation of TUNEL-positive micronuclei and increased the rate of gene amplification (Shimura *et al.*, 1999a), implying that Vpr induces DSBs. Through an analysis with a pulse-field gel electrophoresis on HIV-1 infected cells, we recently detected an altered migration pattern of high-molecular-weight genomic DNA (Tachiwana *et al.*, 2006), also implying that Vpr induces DSBs. Thus, it is now important to clarify whether a cellular response dependent on ATM, a kinase activated selectively by DSBs (O'Connell *et al.*, 2000; Khanna *et al.*, 2001; Shiloh, 2001), is really induced by Vpr, and if so, we need to determine whether Vpr is the major viral protein responsible for ATM activation.

DNA damage is induced by reactive oxygen species, ionizing radiation, and chemicals (Abraham, 2001), and are repaired by homologous recombination (HR) or nonhomologous DNA end-joining (NHEJ) pathways (Khanna and Jackson, 2001; van Gent *et al.*, 2001). Once a DSB is generated, a 3′ single-stranded DNA tail is processed, where replication protein A (RPA) and Rad51, an eukaryotic homologue of the bacterial DNA strand exchange protein RecA (Cromie *et al.*, 2001; West, 2003), accumulate. It was shown that p53 and BRCA2 phosphorylated at serine 3291 bind Rad51 and suppress its HR activity (Dong *et al.*, 2003; Linke *et al.*, 2003; Yoon *et al.*, 2004). Functional BRCA1 and 2 are required when DSBs occur; otherwise, genomic instability is induced, as observed in cancer-prone individuals with mutations of these genes (van Gent *et al.*, 2001; Dong *et al.*, 2003).

In this report, we first show that Vpr induced an ATM-dependent cellular signal. The cellular response under Vpr expression was similar to that caused by X-ray irradiation involving BRCA1, RPA and Rad51. We next demonstrate that Vpr increased the frequency of HR in an ATM-dependent manner. Data support the idea that Vpr induces DSBs. The possible role of Vpr in viral infection and in HIV-1-associated malignant tumor development is discussed.

Results

DSB-induced cellular signals by Vpr

Initially, we examined whether DSB-dependent cellular signals were induced by HIV-1 infection. HT1080 cells were infected with viruses without (R^-) or with wild-type *vpr* (R^+), and an immunohistochemical analysis was performed. As shown in Figure 1a, γ-H2AX accumulated after infection with the R^+ virus (right panels) but not with the R^- virus (Figure 1a, middle panels). Western blot analysis demonstrated a high-level expression of γ-H2AX with the phosphorylation of p53 in cells infected with the R^+ virus (Figure 1b, lanes 4 and 5). Viral concentrations of 50 and 100 ng/ml of p24 were sufficient for the induction of γ-H2AX. In contrast, the R^- virus did not induce p53 phosphorylation, although it slightly increased p53 expression (Figure 1b, lanes 2 and 3).

To characterize the intracellular signals specifically induced by Vpr, we used MIT-23 cells, in which *vpr* mRNA expression was tightly regulated by the tetracycline promoter (Shimura *et al.*, 1999b). In MIT-23 cells, Vpr expression was observed in 48 h after treatment of 3 μg/ml of doxycycline (DOX) (Figure 2a). Under such conditions, we observed focus formation of ATM phosphorylated at serine 1981 (ATM-p) (Figure 2b, upper panels) and γ-H2AX (lower panels). In contrast, focus formation of these molecules was not observed in MIT-23 cells without DOX treatment (left panels). Additionally, we did not detect focus formation of

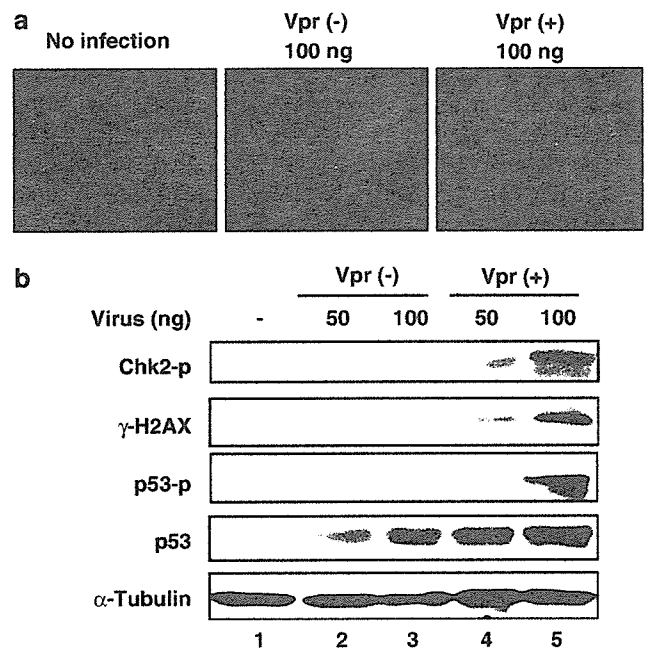

Figure 1 Activation of DSB-induced signaling. (**a**) Focus formation of γ-H2AX in cells infected with R^- or R^+ virus. HT1080 cells were infected with R^- or R^+ virus at the concentration of 100 ng/ml of p24 gag protein. After 48 h of infection, the cells were stained with specific antibody against γ-H2AX. The signals for γ-H2AX are shown as red spots in the nucleus (blue). (**b**) Western blot analysis of proteins involved in the DSB-induced signal pathway. Cell lysates of virus-infected and control cells after 48 h were subjected to analysis. Control cells (lane 1), cells infected with R^- virus (lanes 2 and 3), and cells infected with R^+ virus (lanes 4 and 5) are shown. Two doses of viruses at the concentration of 50 (lanes 2 and 4) and 100 ng/ml of p24 gag protein (lanes 3 and 5) were used. α-Tubulin indicates that the amounts of loaded proteins are not significantly different.

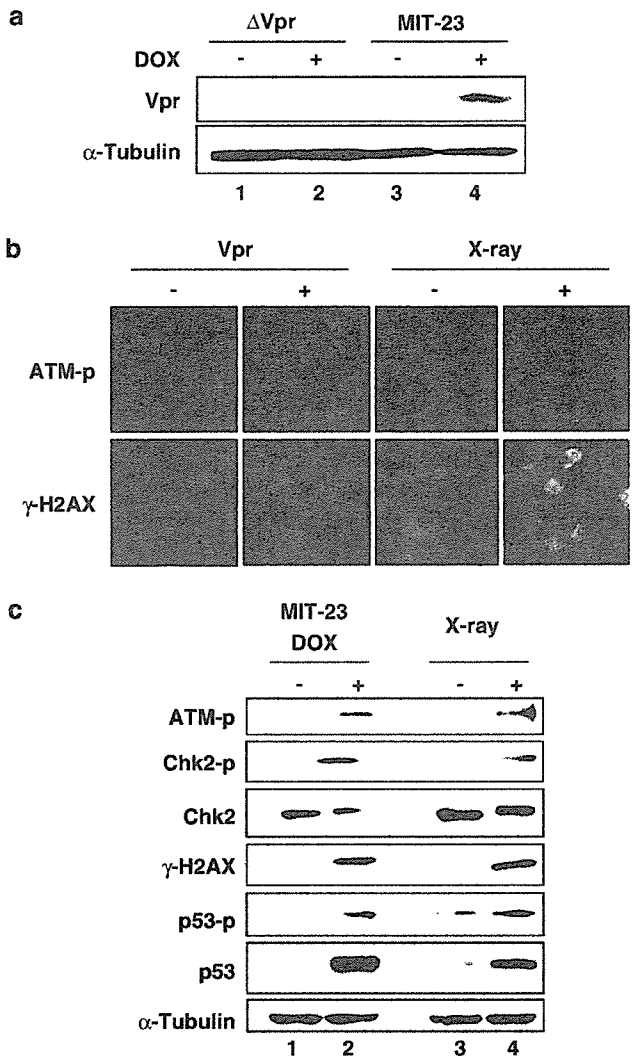

Figure 2 Activation of DSB-induced cellular signaling. (**a**) Expression profiles of Vpr in MIT-23 cells. Vpr expression was induced in 48 h with 3 μg/ml DOX in MIT-23 cells. The Vpr expression level in MIT-23 cells was analysed by Western blotting with the Vpr-specific antibody 8D1. (**b**) Focus formation of phosphorylation of ATM (ATM-p) and γ-H2AX following Vpr expression. The cells were stained with specific antibodies against ATM-p and γ-H2AX. The signals for ATM-p and γ-H2AX are depicted as red spots in the nucleus (blue). (**c**) Western blot analysis of proteins involved in the DSB-induced signal pathway. Cell lysates of MIT-23 cells (lanes 1 and 2) were subjected to analysis. As a positive control, HT1080 cells were irradiated at 7.5 Gy, collected after 30 min, and subjected to analysis.

ATM-p or γ-H2AX in DOX-treated ΔVpr cells, in which only the *vpr* gene was eliminated from vectors that were utilized for the establishment of MIT-23 cells (data not shown). Western blot analysis also detected that DNA-damage-sensing signals were induced by Vpr expression (Figure 2c). Interestingly, Chk2, a substrate of ATM, was highly phosphorylated at threonine 68 by Vpr expression (Figure 2c, lane 2). Additionally, p53 expression as well as its phosphorylation also increased as a downstream response of these molecules. Consistent with the previous report showing that Chk1, a substrate of ATR, is activated by Vpr (Roshal *et al.*, 2003), we observed the presence of the slowly migrating band of Chk1 as its phosphorylated form under Vpr expression (data not shown).

To compare the Vpr-induced DSB-dependent signals with those by X-ray irradiation, HT1080 cells were irradiated with 7.5 Gy of X-rays, and the evoked signals were analysed. As shown in Figure 2b (right panels), X-ray-induced DSBs generated focus formation of ATM-p (Figure 2b, upper panel) and γ-H2AX (lower panel). Additionally, Western blot analysis clearly demonstrated the phosphorylation of both Chk2 and p53 (lane 3 and 4). Data suggest that Vpr-induced DNA-damage signals are quite similar to those triggered by a well-characterized DSB inducer.

Mobilization of cellular factors that are involved in repair of DSBs

To further characterize the molecules activated as a cellular response to Vpr-induced DSBs, we investigated BRCA1, RPA and Rad51 mobilized for repair of DSBs (West, 2003). As shown in Figure 3, the immunohistochemical analysis carried out under Vpr expression clearly detected focus formation of these molecules (Figure 3). In contrast, control cells did not show remarkable modification of these molecules. Again, X-ray irradiation also induced the same modification of the molecules (Figure 3, right panels).

It has been proposed that during the DSB repair process, Rad51 is released from a complex of p53 and becomes competent for HR (Linke *et al.*, 2003; Bertrand *et al.*, 2004). To address this possibility, we compared the physical association of Rad51 and p53 in the insoluble chromatin fraction before and after the induction of Vpr expression. The interaction of these molecules was eliminated following Vpr expression (Figure 4a, lanes 3 and 4; arrow). The level of the complex formation of p53 and Rad51 decreased by 35% compared to the control. This finding is reproducibly observed, implying the possibility that Vpr binds either Rad51 or p53 and ceases their interaction. We examined the direct interaction of Vpr and Rad51 by using recombinant proteins, but did not obtain positive results (data not shown). As it has been shown that Vpr does not interact with p53 (Sawaya *et al.*, 1998), the mechanism of dissociation of p53 and Rad51 in Vpr-expressing cells remains to be clarified.

We also compared this molecular change with that induced by X-ray irradiation. HT1080 cells were irradiated, and the subsequent change of the interaction of Rad51 and p53 was examined. As observed in Figure 4a, the interaction between Rad51 and p53 in the insoluble chromatin fraction was also abolished (Figure 4b, compare lanes 3 and 4, arrow). Data suggest that Vpr modifies Rad51 in the same way as X-ray irradiation.

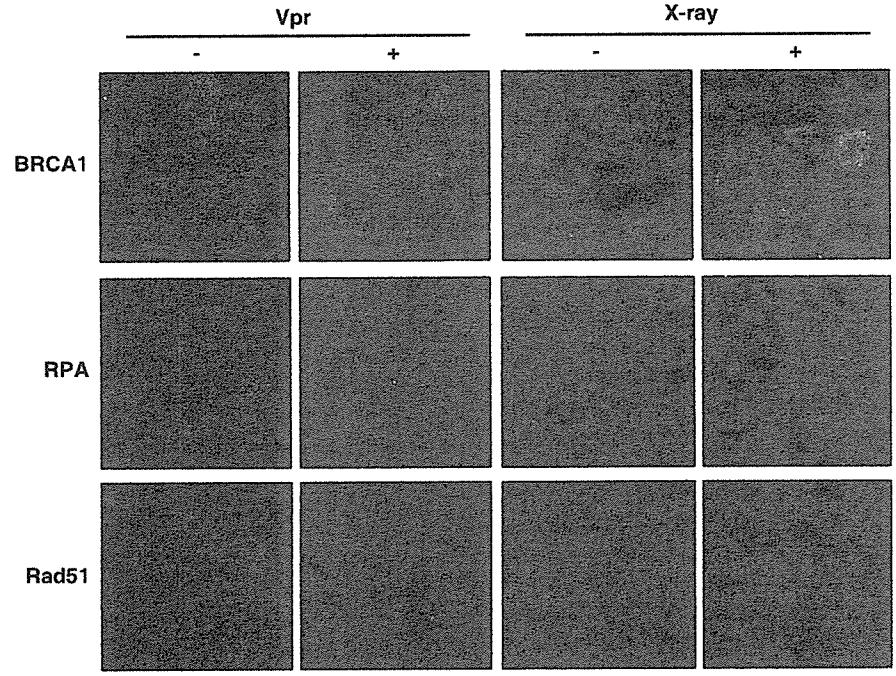

Figure 3 Involvement of BRCA1, RPA and Rad51 in Vpr-induced signaling. MIT-23 cells were cultured in the presence or absence of 3 μg/ml DOX for 48 h. Focus formations of BRCA1, RPA and Rad51 during Vpr expression are shown. These signals are visualized as red spots in the nucleus (blue).

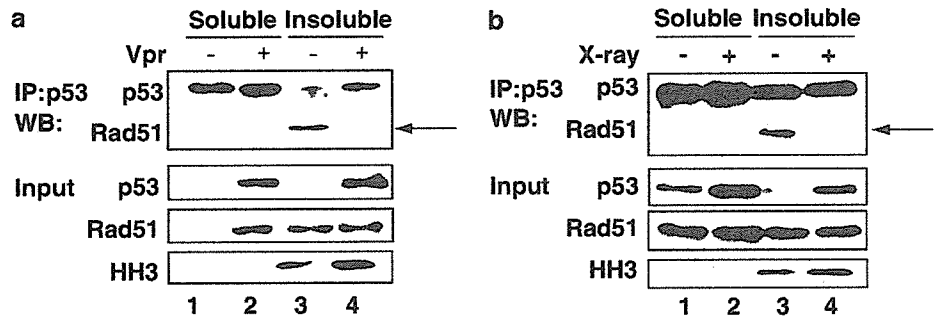

Figure 4 Dissociated interaction of p53 and Rad51 in a chromatin fraction during Vpr expression. The lysates of the soluble (lanes 1 and 2) and insoluble chromatin fractions (lanes 3 and 4) subjected to analysis. Proteins that were immunoprecipitated (IP) with the anti-p53 antibody (αp53) were analysed by Western blot analysis (WB) with the αp53 and αRad51 antibodies, respectively. Input lysates were also analysed by the same antibodies and αhistone H3 (HH3). The cell lysate with (lanes 2 and 4) or without (lanes 1 and 3) Vpr expression are shown (**a**). The same analysis was performed on X-ray irradiated cells (**b**). Arrowheads indicate Rad51 recovered by αp53 antibody.

Increased rate of HR by Vpr

DSBs must be correctly repaired, or genome integrity cannot be maintained (West, 2003). As Vpr induces DSBs and cellular factors such as Rad51 and BRAC1 are mobilized under Vpr expression, we hypothesized that the rate of HR increased in Vpr-expressing cells. To measure the rate of HR, we first utilized a system invented by Slebos and Taylor (2001) that could monitor extrachromosomal recombination within a plasmid DNA (pBHRF). pBHRF contains a truncated EBFP cassette, which forms a functional EGFP following intramolecular HR (Slebos and Taylor, 2001). We co-transfected HT1080 with pBHRF and a plasmid DNA encoding Vpr and examined the effects of Vpr on HR. After 72 h of transfection, the EGFP- and EBFP-positive cells were counted by flow cytometry (Figure 5a, regions a and b, respectively). Then, the frequency of HR was calculated as a ratio of number of cells positive for EGFP and EBFP. It increased about 2.5-fold by co-transfection of a plasmid encoding Vpr. Vpr-induced enhancement of HR was reproducibly observed ($P<0.05$), and the representative results are shown in Figure 5b.

Although the experiments with pBHRF strongly suggested that Vpr increases HR, it has been demonstrated that an extrachromosomal HR does not correlate with intrachromosomal HR. Waldman and Liskay (1987) clearly demonstrated that the frequency of

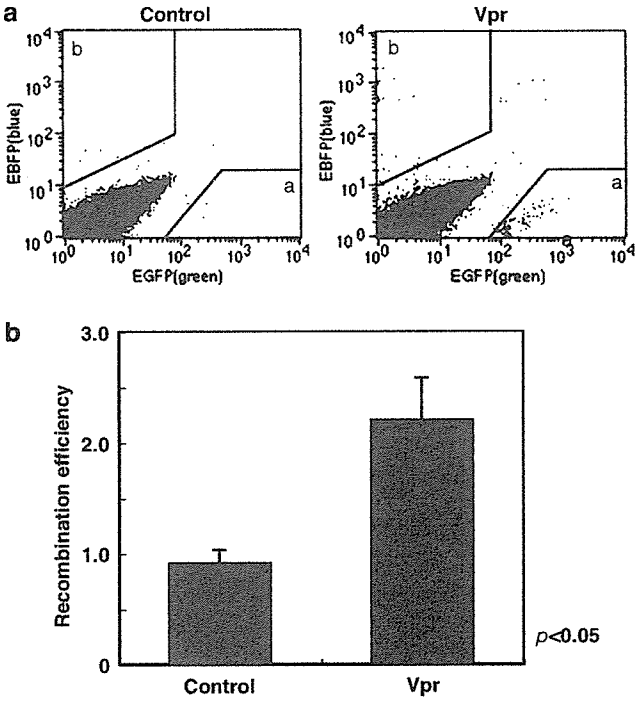

Figure 5 Increased rate of extrachromosomal HR by Vpr. (**a**) A representative result of three independent experiments with pBHRF. HT1080 cells were co-transfected with pBHRF and pcDNA3.1/Vpr (see Materials and methods section). The cells were subjected to analysis by flow cytometry after 72 h. Regions a and b were tentatively determined in a control sample. These indicate the areas where cells positive for EGFP (region a) or EBFP (region b) were not present in untreated samples. After treatment cell numbers in these areas were counted and compared. (**b**) Increase of GFP-positive cells by Vpr. The ratio of GFP-positive cells to BFP-positive cells, which are indicative of HR frequencies (Slebos and Taylor, 2001), were counted. Each sample was analysed twice in triplicate; bars ± s.d.

extrachromosomal and intrachromosomal recombination rates are differentially influenced by the mismatch of the nucleotides. To measure the rate of intrachromosoml HR under Vpr expression correctly, we prepared stable transfectants derived from HT1080 cells that had been introduced with pDR-GFP. pDR-GFP is a reporter construct that will generate an intact EGFP gene by gene conversion after digestion with a rare cutting enzyme, I-*Sce*I (Pierce *et al*., 1999). We obtained two independent transfectants, HT/DR-GFP-1 and -2, that possessed an integrated exogenous plasmid DNA competent for a short tract gene conversion (Supplementary information 1a) (Pierce *et al*., 1999). Then, HT/DR-GFP cells were infected with adenoviruses of either Adβgal or Ad-SceI-NG and subjected to analysis of GFP-positive cells after 72 h. After infection with Ad-SceI-NG, both clones gave increased numbers of GFP-positive cells (about 0.5%) (Supplementary information 1b and c). In contrast, Adβgal, control adenovirus, induced very few cells positive for GFP (<0.1%) (Supplementary information 1b and c).

We then examined the influence of Vpr on the rate of HR. First, we introduced a plasmid DNA encoding Vpr or its control plasmid DNA, but it was not possible to assess the effects of Vpr correctly because transfection of plasmid DNA by itself influenced the rate of HR (data not shown). It has been well reported that Vpr enters cells and expresses its biological activity when added to the cell culture (Jenkins *et al*., 1998; Henklein *et al*., 2000; Huang *et al*., 2000; Taguchi *et al*., 2004). These observations encouraged us to perform the experiments by adding Vpr to cells exogenously with subsequent measurement of GFP-positive cells. We prepared a recombinant Vpr (rVpr) (Hoshino *et al*., submitted), and we first checked whether exogenously added rVpr induces DSB-triggered cellular response. rVpr (50 ng/ml; 3.7 nM) added to the medium induced DSB-dependent signals (Figure 6a), whereas glutathione *S* transferase (GST), an irrelevant recombinant protein that was expressed in bacteria and purified, did not (right panels). Interestingly, the addition of the ATM inhibitor KU55937 abolished rVpr-induced focus formation of ATM-p and γ-H2AX (Figure 6a).

When rVpr was added to HT/DR-GFP-1 (clone-1), HR especially after infection with Ad-SceI-NG-infected was definitely enhanced (about 1.5%), whereas it was not remarkably changed by the addition of GST (Figure 6b and c, left panel). The difference in GFP-positive numbers after treatment with rVpr and GST was statistically significant ($P<0.01$). As more striking evidence, the addition of KU55933 significantly attenuated the increased number of GFP-positive cells caused by rVpr (Figure 6c, right panel) ($P<0.01$). Data indicate that ATM is a critical molecule for the Vpr-induced enhancement of HR.

Discussion

Vpr induces DSBs and enhances HR

In this study, we showed that Vpr activates the ATM-dependent signal pathway involving Chk2 phosphorylation with focus formation of Rad51, BRCA1 and γ-H2AX. We previously reported that Vpr increases the rate of gene amplification (Shimura *et al*., 1999a), and a subsequent analysis by fluorescence *in situ* hybridization of amplified DNA suggested that a bridge-breakage fusion cycle, possibly triggered by DSBs (Ishizaka *et al*., 1995), was a relevant mode of Vpr-induced gene amplification. Data shown in the present study well supports our expectation that Vpr enhances gene amplification by causing DSBs (Shimura *et al*., 1999a).

We observed that the frequency of HR increased in response to Vpr. We examined the rate of HR by two systems measuring extrachromosomal recombination (Slebos and Taylor, 2001) and intrachromosomal recombination (Pierce *et al*., 1999). Both systems detect cells that are positive for GFP generated by gene conversion. Although it has been claimed that these two modes of HR do not always equally detect cellular recombinogenic conditions, our present data revealed that both systems detected the effects of Vpr on HR. It is interesting to note that the intrachromosomal recombination system used in the current study detects HR at

the specific site in the genome, where DSB is induced by expressing I-*Sce*I, a rare-cutting enzyme (Anglana and Bacchetti, 1999). We used two cell lines, both of which contained reporter constructs that were competent for a short tract gene conversion (Pierce *et al*., 1999; Supplementary information 1), and we reproducibly detected enhancement of HR after treatment with Vpr. Data suggest that Vpr has an indirect effect on HR, indicating that DBSs at one locus contribute to trans-activation of HR at a different site.

In response to Vpr-induced DSBs, BRCA1 and RPA accumulated as foci (Figure 2b), and the association of Rad51 and p53 in the chromatin fraction was eliminated (Figure 3a and b). It has been reported that p53 associates with several proteins including BLM, BRCA1, BRCA2, Rad52 and RPA (Yamaguchi-Iwai

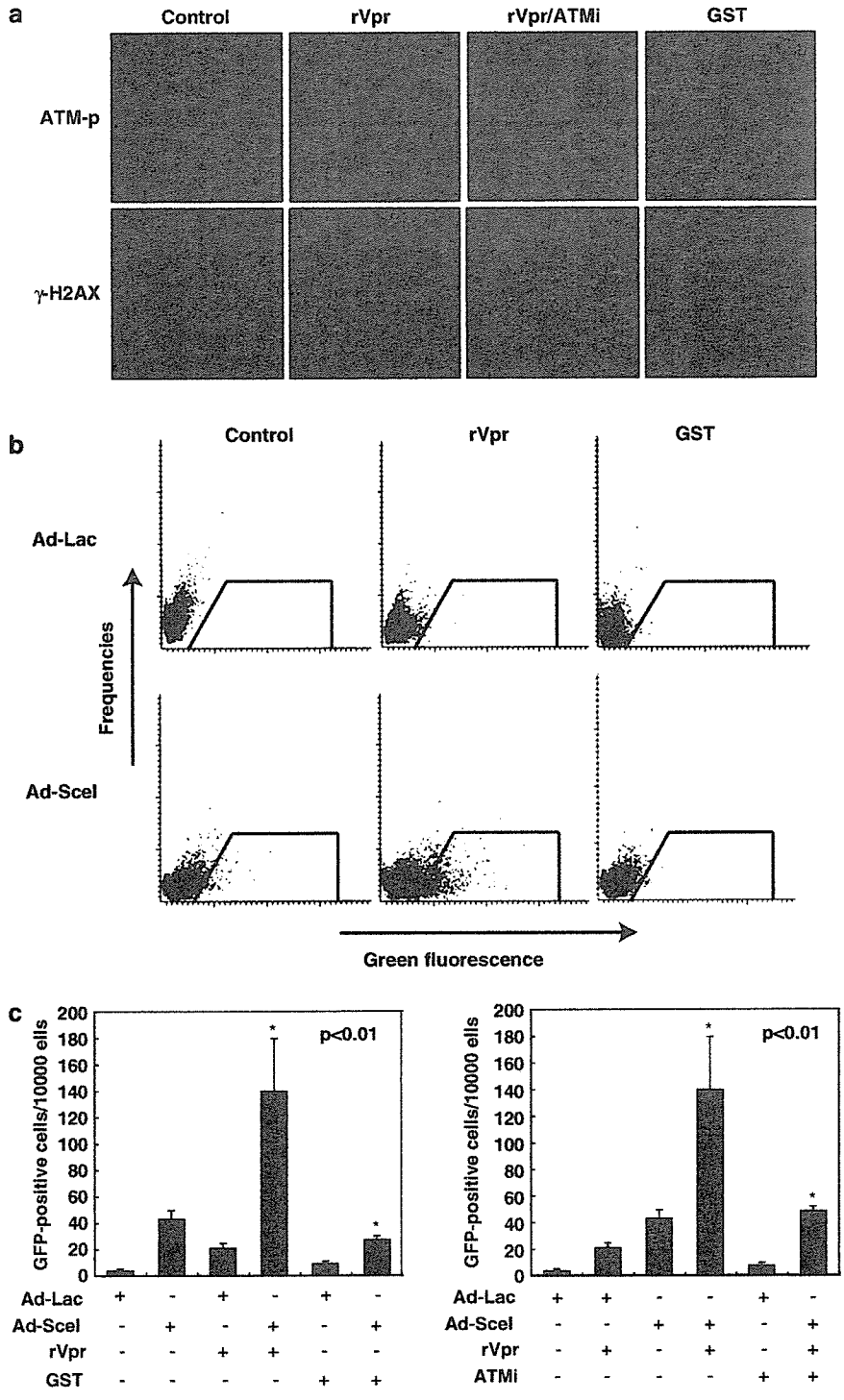

et al., 1998; Marmorstein *et al.*, 1998; Zhang *et al.*, 1998; Linke *et al.*, 2003; Sengupta *et al.*, 2003) and inhibits the Rad51-dependent HR (Cromie *et al.*, 2001; Linke *et al.*, 2003). When DSBs were induced, the association of p53 and Rad51 was prevented by an unknown mechanism. As the reduction of Rad51 and p53 interaction was also observed after irradiation (Figure 3c), it is likely that the Vpr-activated DNA-damage signaling overlaps with the cellular signals evoked by irradiation.

Biological relevance of Vpr-induced DSBs and HR for HIV-1 infection

Vpr expression enhances the rate of HR, but several reports suggest that NHEJ rather than HR contributes to viral infection (Daniel *et al.*, 1999; Li *et al.*, 2001; Jeanson *et al.*, 2002; Lau *et al.*, 2005). Additionally, Rad52, a cellular component of HR, was shown to work as a suppressive factor for HIV-1 transduction (Lau *et al.*, 2004). Together with data that the deletion of genes involved in HR, such as XRCC2 or XRCC3, did not alter the rate of viral integration (Chan *et al.*, 2004), it seems that upregulation of HR by Vpr does not by itself contribute to viral transduction.

In contrast, chemical compounds that generate DSBs increase the rate of integration of viral DNA into the host genome (Groschel and Bushman, 2005). This phenomenon has been explained by delayed progression at the G2/M phase due to DSBs. Additionally, caffeine and caffeine-related methylxanthines are known to impair HIV-1 infection (Nunnari *et al.*, 2005), and an ATM inhibitor, KU55933, is known to decrease the integration of viral DNA into host genome (Lau *et al.*, 2005). These observations suggest that a DSB-induced cellular signal, not HR, is important for viral integration, and that Vpr-induced DSB contributes to efficient viral integration in an ATM-dependent manner. An important issue to clarify is how cellular signals activated by ATM contribute to increased viral integration.

Possible mechanism of Vpr-induced DSBs and cell cycle abnormality

The mechanism of Vpr-induced DSBs is presently obscure. In the previous work, we showed that DSBs are induced by incubating isolated nuclei with purified recombinant Vpr protein (Tachiwana *et al.*, 2006). A purified Vpr possessed DNA binding activity, but it did not show any nuclease activity or activity of nicking DNAs. Additionally, Vpr is present in the chromatin fraction (Ishizaka, unpublished results, Lai *et al.*, 2005), implying the possibility that Vpr induces DSBs by modifying a chromatin structure to allow nucleases easy access. Another possibility is that Vpr associates with uncharacterized nuclease and recruits its activity to the vicinity of chromosomes. Studies are ongoing to identify cellular factor(s) that facilitate recruitment of Vpr to chromatin and induction of DSBs.

It is commonly accepted that Vpr-induced cell cycle abnormality is observed at the G2/M phase but not at the G1/S phase (Mahalingam *et al.*, 1998). Actually, we observed cellular accumulation at the G2/M phase in MIT-23 cells when Vpr expression was initiated (Shimura *et al.*, 1999b). Our present observation on the activation of ATM-dependent signal pathway by Vpr envisages that Vpr-induced cell cycle abnormality depends on ATM activation. A recent study, however, has shown that the ATR–Chk1 pathway, but not ATM–Chk2, is necessary for Vpr-induced G2 arrest (Roshal *et al.*, 2003; Zimmerman *et al.*, 2004). One possible explanation is that DSB-induced G2 arrest, for example, by X-ray irradiation largely depends on ATR-dependent signaling (Brown and Baltimore, 2003). The molecular linkage between ATM activation by Vpr and Vpr-induced cell cycle abnormality, however, needs to be carefully investigated.

Impact of Vpr-induced DSBs on the mechanism of tumor development in HIV-1-positive patients

We showed that DSBs and an increased rate of HR were induced when rVpr was added to the culture medium exogenously (Figure 6). Recently, we also found that Vpr is present in serum of HIV-1-positive patients (Levy *et al.*, 1994) at the concentration of about 0.7 nM (Hoshino *et al.*, submitted). In the current study, we used 3.7 nM of rVpr to obtain the definite activity inducing DSBs, but it would be possible that the high concentration of Vpr is present in the foci of HIV-1 infection, suggesting that DSBs can be generated in the cells within HIV-1-positive patients. The finding that Vpr is present in serum impacts the understanding of the mechanism of tumor development in HIV-1 positive patients. As reported by Biggar *et al.*, the relative risk of

Figure 6 Increased rate of intrachromosomal HR after treatment with rVpr. (**a**) Focus formation of γ-H2AX in cells treated with or without rVpr. HT1080 cells were incubated for 48 h in the presence of 3.7 nM of rVpr (see Materials and methods section), and subjected to immunohistochemical analysis by antibodies against ATM-p and γ-H2AX. Effects of KU55933 on rVpr-induced focus formation of these molecules are shown. As controls, the effects of the same concentration of GST, as an irrelevant bacteria-derived recombinant protein, are depicted (right panel). Their signals are shown as red spots in the nucleus (blue). (**b**) Effects of rVpr on HR. HT/DR–GFP cells (clone-1) were infected with Adβgal or Ad–SceI–NG with or without the addition of 3.7 nM of rVpr (middle panel). As a control, the same amount of GST was added to the culture (right panel). A region where no GFP-positive cells were present in control sample was first determined (upper left panel). Then numbers of cells in the gated areas were counted in the specimens after viral infection with or without treatment of recombinant proteins. (**c**) Vpr-induced increase of HR depends on ATM. Data obtained in Figure 6b were summarized (left panel). The addition of rVpr reproducibly enhanced the number of GFP-positive cells ($P<0.01$). Effects of ATM inhibitor (ATMi) were analysed by the same procedures shown in Figure 6b (right panel). KU55933 (ATMi) was added at a concentration of 1 mM at the same time that rVpr was added. As a control, the corresponding amount of dimethylsulfoxide (final concentration: 0.1% volume), which was used as a solvent for the compound, was included. ATMi significantly inhibited the rate of HR ($P<0.01$).

malignancy in AIDS patients was estimated to be 60- to1000-fold higher than healthy controls (Mayer *et al.*, 1995; Biggar *et al.*, 1996; Straus, 2001). Although it has been thought that an impaired cellular immunity under AIDS conditions permits the development of tumorigenesis (Knowles, 2003), recent observations indicate that non-AIDS-defining malignancies, tumors found in HIV-1-positive patients who have no deteriorated cellular immunity, are frequently observed in HIV-1-positive patients (Herida *et al.*, 2003; Burgi *et al.*, 2005; Lim and Levine, 2005). As antiretroviral therapy can effectively protect patients from severe infectious diseases (Chadburn and Cesarman, 1997; Elenitoba-Johnson and Jaffe, 1997), development of malignant tumors will be a critical prognostic factor of HIV-1 positive patients in the future. More precise study is required to clarify the molecular linkage of Vpr and malignant transformation.

Materials and methods

Cell culture and establishment of HT/DR-GFP

HT1080, a human fibrosarcoma cell line (JCRB9113; the Healthy Science Research Resources Bank), and its sublines were maintained at 37°C and 5% CO_2 in Dulbecco's modified Eagles medium (D-MEM) that was supplemented with 10% fetal bovine serum (FBS). The MIT-23 cell line was derived from HT1080 cells, in which Vpr expression is controlled by a tetracycline promoter, as described by Shimura *et al.* (1999b). For Vpr induction, 3 μg/ml DOX (Sigma, St Louis, MO, USA) was used. To obtain HT/DR-GFP, HT1080 cells were transfected with an inactive GFP expression cassette plasmid (pDR-GFP) and selected by puromycin (1 μg/ml), and clonal cell lines were established.

HIV infection

We used pseudotyped viruses that were defective for an envelope protein with *vpr* (R^+) or without *vpr* (R^-). HIV vectors were produced by transient transfection of 293T cells (Tokunaga *et al.*, 2001; Shimura *et al.*, 2005). The pNL-Luc-E^-R^+ or pNL-Luc-E^-R^- plasmid was co-transfected with pHIT/G using the transfection reagent Fugene-6 (Roche, Tokyo, Japan). Virus supernatants were collected at 48 h post-transfection. The harvested supernatants were centrifuged at 120 *g* for 5 min and stored at −80°C. Viral titers were measured by p24 ELISA (ZeptoMetrix). The virus was diluted in D-MEM supplemented with 10% FBS and used to infect HT1080 cells at a multiplicity of infection (MOI) of 0.8, which yielded about 80% of cells that were positive for luciferase expression (data not shown).

Protein analyses

The cells were washed with phosphate-buffered saline (PBS) and resuspended in radio-immunoprecipitation assay buffer composed of 50 mM Tris-HCl, 1% NP-40, 0.25%. sodium deoxycholate, 150 mM NaCl, 1 mM EGTA, 1 mM phenylmethysulfonyl fluoride, 1 μg/ml protease inhibitor mix, 1 mM Na_2VO_3 and 1 mM NaF. The cell suspension was sonicated. To fractionate chromatin fractions, cells were suspended in Buffer N (15 mM Tris-HCl (pH 7.5), 60 mM KCl, 15 mM NaCl, 5 mM $MgCl_2$, 1 mM $CaCl_2$, 1 mM DTT, 2 mM Na_2VO_3, 250 mM sucrose, protease inhibitors) with 0.6% NP-40. Cells were incubated on ice for 5 min followed by centrifugation (2000 *g*) to separate cytoplasmic proteins from nuclei. Isolated nuclei were then washed twice with Buffer N followed by resuspension in Lysis buffer (10 mM PIPES (pH 6.5), 10 mM EDTA, protease inhibitors) and centrifugation (6000 *g*) to extract soluble nuclear proteins. Finally, chromatin was resuspended in Lysis buffer and shared by sonication on ice to extract chromatin-bound proteins. The protein concentration was determined using the BCA protein assay reagent kit (Pierce). A 100-μg aliquot of protein from each cell extract was separated on 10% SDS–PAGE. Specific primary antibodies of p53 (Calbiochem), Chk2, ATM-S1981 (ATM-p), H2AX-S139 (γ-H2AX) and histone H3 (Upstate), Chk2-T68 (Chk2-p) and p53-S15 (p53-p) (Cell Signaling) were used for analysis. A monoclonal antibody to Vpr, 8D1 (IgG2a) was raised by immunization of a full-length Vpr peptide (Peptide Institute).

Immunoprecipitation was performed using 500 μg of protein mixed with 2 μg of anti-p53 protein-specific IgG-beads. Ternary complexes of protein A–antibody–antigen were collected by centrifugation and washed three times. The immunoprecipitates were subjected to SDS–PAGE followed by Western blot analysis. To obtain a rabbit antibody to RAD51, the human Rad51 protein was expressed as a recombinant protein in the *Escherichia coli* strain JM109 (DE3) (Kagawa *et al.*, 2001), and was purified as described previously (Kurumizaka *et al.*, 1999). Detection of target proteins was with an enhanced chemiluminescence detection system (Amersham Biosciences).

Immunostaining

The cells were washed with PBS and fixed with 2% paraformaldehyde in PBS and ice-cold methanol. The fixed cells were permeabilized with 0.2% Triton X-100 in PBS for 5 min. After treatment with PBS containing 10% goat serum for 30 min, the cells were incubated with primary antibodies that included rabbit polyclonal antibodies against Rad51 (1:400), mouse monoclonal antibodies against ATM-p (1:100) and γ-H2AX (1:100) (Upstate) and mouse monoclonal antibodies against BRCA1 (1:300) and RPA (1:1000) (Lab Vision). After 1 h of incubation at 37°C, secondary antibodies conjugated with Alexa 546 (1:1000; Molecular Probes, Eugene, OR, USA) were added for 1 h at 37°C. The slides were mounted in an anti-fade solution (KPL) and analysed by fluorescence microscopy.

Homologous recombination assay

The rate of extrachromosomal HR was assessed as previously described (Slebos and Taylor, 2001). HT1080 cells were co-transfected with pBHRF and pcDNA3.1/Vpr or pcDNA3.1 (Invitrogen). pBHRF encodes both a truncated GFP and full-length BFP. In the absence of HR, only BFP is expressed. However, HR between the BFP and truncated GFP results in the creation of a functional GFP. The green and blue fluorescence levels were examined simultaneously using a Vantage flow cytometer (Becton-Dickinson) equipped with a 488-argon laser (GFP) and a UV (350–360 nm) laser (BFP). *vpr* was derived from a NL4-3 clone (Adachi *et al.*, 1986). Each experiment was performed at least three times, and statistical analysis was carried out by Student's *t*-test.

The rate of intrachromosomal HR was assessed as reported in human glioma cells (Pierce *et al.*, 1999). Upon infection with Ad-I-Sce-I, a kind gift from Dr F Graham (McMaster University, Canada) or Ad-Lac8 (a gift from Dr I Saito, Tokyo University) as a control, GFP-positive cells as a result of HR were analysed. KU55933, a gift from Dr M O'Connor (KuDOS Pharmaceuticals, England), was dissolved in dimethylsulfoxide (DMSO). GFP was analysed with laser scanning cytometer

(LSC; Olympus, Tokyo, Japan) (Huang *et al.*, 2006). Cells cultured in cover slide were immersed in 0.2% Triton X-100 in PBS for 10 min. The slides were then incubated with anti-GFP antibody (1:100; Molecular Probes) before adding Alexa Fuor 488 conjugated secondary antibody (1:400; Molecular Probes). Green fluorescence emission was measured with LSC. The integrated fluorescence was measured in 10 000 cells for each sample. Each experiment was repeated three times, and statistical significance was examined.

Expression and purification of rVpr

rVpr was expressed in BL-21 codon plus (Stratagene) as a GST fusion protein and purified using glutathione column chromatography, as described (Hoshino *et al.*, submitted). Vpr eluted after precision treatment was applied to an affinity column coupled with a monoclonal antibody to Vpr, 8D1. After washing, Vpr was eluted with 100 mM Hepes buffer (pH 2.5), and immediately neutralized with 1 M Hepes buffer (pH 8.0). The concentration of rVpr was measured by an enzyme-linked immunosorbent assay version-1 by using two antibodies against Vpr, a monoclonal antibody (8D1), and a polyclonal antibody raised against a peptide of the carboxy-terminus of Vpr (IBL).

Acknowledgements

We are grateful to Dr T Takemori (National Institute of Infectious Diseases, Japan) to help for analysis by a Vantage flow cytometer. We also thank to Riken BRC for control adenovirus, AxCALac8, and HT1080 cells. Drs Slebos (National Institute of Environmental Health Science, USA), Jasin M (Memorial Sloan-Kettering Cancer Center, USA), Graham F (McMaster University, Canada), and Saito I (Institute of Medical Sciences, of Tokyo University, Japan) kindly provided us with pBHRF, pDR-GFP, adenovirus of I-*Sce*I, and AxCALac8, respectively. We also thank to O'Connor M (KuDOS pharmaceuticals, England) for KU55933. This work was supported by a Grant-in-Aid for Scientific Research from the Ministry of Health, Labor and a Grant for research on Health Sciences focusing on Drug Innovation. Dr Nakai-Murakami is a research resident supported by the Japan Health Sciences Foundation.

References

Abraham RT. (2001). *Genes Dev* **15**: 2177–2196.
Anglana M, Bacchetti S. (1999). *Nucleic Acids Res* **27**: 4276–4281.
Bartz SR, Rogel ME, Emerman M. (1996). *J Virol* **70**: 2324–2331.
Bertrand P, Saintigny Y, Lopez BS. (2004). *Trends Genet* **20**: 235–243.
Biggar RJ, Rosenberg PS, Coté T, Multistate AIDS/Cancer Match Study Group. (1996). *Int J Cancer* **68**: 754–758.
Brown EJ, Baltimore D. (2003). *Genes Dev* **17**: 615–628.
Bukrinsky M, Adzhubei A. (1999). *Rev Med Virol* **9**: 39–49.
Burgi A, Brodine S, Wegner S, Milazzo M, Wallace MR, Spooner K *et al.* (2005). *Cancer* **104**: 1505–1511.
Chadburn A, Cesarman E, Knowles DH. (1997). *Semin Diagn Pathol* **14**: 15–26.
Cromie GA, Connelly JC, Leach DRF. (2001). *Mol Cell* **8**: 1163–1174.
Daniel R, Greger JG, Katz RA, Taganov KD, Wu X, Kappes JC *et al.* (2004). *J Virol* **78**: 8573–8581.
Daniel R, Kao G, Tagarov K, Greger JG, Favorova O, Merkel G *et al.* (2003). *Proc Natl Acad Sci USA* **100**: 4778–4783.
Daniel R, Katz RA, Skalka AM. (1999). *Science* **284**: 644–647.
Daniel R, Marusich E, Argyris E, Zhao RY, Skalka AM, Pomerantz RJ. (2005). *J Virol* **79**: 2058–2065.
Dong Y, Hakimi MA, Chen X, Kumaraswamy E, Cooch NS, Godwin AK *et al.* (2003). *Mol Cell* **12**: 1087–1099.
Elder RT, Benko Z, Zhao Y. (2002). *Front Biosci* **7**: d349–d357.
Elenitoba-Johnson KS, Jaffe ES. (1997). *Semin Diagn Pathol* **14**: 35–47.
Goh WC, Rogel ME, Kinsey CM, Michael SF, Fultz PN, Nowak MA *et al.* (1998). *Nat Med* **4**: 65–71.
Groschel B, Bushman F. (2005). *J Virol* **79**: 5695–5704.
He J, Choe S, Walker R, Di Marzio PD, Morgan DO, Landau NR. (1995). *J Virol* **69**: 6705–6711.
Henklein P, Bruns K, Sherman MP, Tessmer U, Licha K, Kopp J *et al.* (2000). *J Biol Chem* **275**: 32016–32026.
Herida M, Mary-Krause M, Kaphan R, Cadranel J, Poizot-Martin IP, Rabaud C *et al.* (2003). *J Clin Oncol* **21**: 3447–3453.
Hoshino S, Sun B, Shimura M, Konishi M, Taguchi T, Segawa T *et al.* (2006). *submitted.*
Huang M-B, Weeks O, Zhao L-J, Saltarelli M, Bond VC. (2000). *J Neuro Viol* **6**: 202–220.
Huang X, Kurose A, Tanaka T, Traganos F, Dai W, Darzynkiewicz Z. (2006). *Cytometer A* **69A**: 222–229.
Ishizaka Y, Chernov MV, Burns CM, Stark GR. (1995). *Proc Natl Acad Sci USA* **92**: 3224–3228.
Yamaguchi-Iwai Y, Sonoda E, Buerstedde J-M, Bezzubova O, Morrison C, Takata M *et al.* (1998). *Mol Cell Biol* **18**: 6430–6435.
Jeanson L, Subra F, Vaganay S, Hervy M, Marangoni E, Bourhis J *et al.* (2002). *Virology* **300**: 100–108.
Jenkins Y, McEntee M, Weis K, Greene WC. (1998). *J Cell Biol* **143**: 875–885.
Kagawa W, Kurumizaka H, Ikawa S, Yokoyama S, Shibata T. (2001). *J Biol Chem* **276**: 35201–35208.
Khanna KK, Jackson SP. (2001). *Nat Genet* **27**: 247–254.
Khanna KK, Lavin MF, Jackson SP, Mulhern TD. (2001). *Cell Death Differ* **8**: 1052–1065.
Knowles DM. (2003). *Hematol Oncol Clin N Am* **17**: 785–820.
Kurumizaka H, Aihara H, Kagawa W, Shibata T, Yokoyama S. (1999). *J Mol Biol* **291**: 537–548.
Lai M, Zimmerman ES, Planelles V, Chen J. (2005). *J Virol* **79**: 15443–15451.
Lau A, Kanaar R, Jackson SP, O'Connor MJ. (2004). *EMBO J* **23**: 3421–3429.
Lau A, Swinbank KM, Ahmed PS, Taylor DL, Jackson SP, Smith GCM *et al.* (2005). *Nat Cell Biol* **7**: 493–500.
Laurence J, Astrin SM. (1991). *Proc Natl Acad Sci USA* **88**: 7635–7639.
Levy DN, Refaeli Y, MacGregor RR, Weiner DB. (1994). *Proc Natl Acad Sci USA* **91**: 10873–10877.
Li L, Olvera JM, Yoder KE, Mitchell RS, Butler SL, Lieber M *et al.* (2001). *EMBO J* **20**: 3272–3281.
Lim ST, Levine AM. (2005). *Curr HIV/AIDS Rep* **2**: 146–153.
Linke SP, Sengupta S, Khabie N, Jeffries BA, Buchhop S, Miska S *et al.* (2003). *Cancer Res* **63**: 2596–2605.
Mahalingam S, Ayyavoo V, Patel M, Kieber-Emmons T, Kao GD, Muschel RJ *et al.* (1998). *Proc Natl Acad Sci USA* **95**: 3419–3424.
Marmorstein LY, Ouchi T, Aaronson SA. (1998). *Proc Natl Acad Sci USA* **95**: 13869–13874.

Mayer V, Ebbesen P, Zachar V. (1995). *Eur J Cancer Prev* **4**: 211–212.
Nunnari G, Argyris E, Fang J, Mehlman KE, Pomerantz RJ, Daniel R. (2005). *Virology* **335**: 177–184.
O'Connell MJ, Walworth NC, Carr AM. (2000). *Trends Cell Biol* **10**: 296–303.
Pierce AJ, Johnson RD, Thompson LH, Jasin M. (1999). *Gene Dev* **13**: 2633–2638.
Roshal M, Kim B, Zhu Y, Nghiem P, Planelles V. (2003). *J Biol Chem* **278**: 25879–25886.
Sawaya BE, Khalili K, Mercer WE, Denisova L, Amini S. (1998). *J Biol Chem* **273**: 20052–20057.
Sengupta S, Linke SP, Pedeux R, Yang Q, Farnsworth J, Garfield SH *et al.* (2003). *EMBO J* **22**: 1210–1222.
Shiloh Y. (2001). *Curr Opin Genet Dev* **11**: 71–77.
Shimura M, Onozuka Y, Yamaguchi T, Hatake K, Takaku F, Ishizaka Y. (1999a). *Cancer Res* **59**: 2259–2264.
Shimura M, Tanaka Y, Nakamura S, Minemoto Y, Yamashita K, Hatake K *et al.* (1999b). *FASEB J* **13**: 621–637.
Shimura M, Tokunaga K, Konishi M, Sato Y, Kobayashi C, Sata T *et al.* (2005). *AIDS* **19**: 1434–1438.
Slebos RC, Taylor JA. (2001). *Biochem Biohpys Res Commun* **281**: 212–219.
Straus DJ. (2001). *Curr Oncol Rep* **3**: 260–265.
Tachiwana H, Shimura M, Nakai-Murakami C, Tokunaga K, Takizawa Y, Sata T *et al.* (2006). *Cancer Res* **66**: 627–631.
Taguchi T, Shimura M, Osawa Y, Suzuki Y, Mizoguchi I, Niino K *et al.* (2004). *Biochem Biophys Res Commun* **320**: 18–26.
Tokunaga K, Greenberg ML, Morse MA, Cumming RI, Lyerly HK, Cullen BR. (2001). *J Virol* **75**: 6776–6785.
van Gent DC, Hoeijmakers JHJ, Kanaar R. (2001). *Nat Rev Genet* **2**: 196–206.
Waldman AS, Liskay RM. (1987). *Proc Natl Acad Sci USA* **84**: 5340–5344.
West SC. (2003). *Nat Rev Mol Cell Biol* **4**: 1–11.
Yoon D, Wang Y, Stapleford K, Wiesmüller L, Chen J. (2004). *J Mol Biol* **336**: 639–654.
Yuan H, Kamata M, Xie Y-M, Chen ISY. (2004). *J Virol* **78**: 8183–8190.
Zhang H, Somasundaram K, Peng Y, Tian H, Zhang H, Bi D, Weber BL *et al.* (1998). *Oncogene* **16**: 1713–1721.
Zimmerman ES, Chen J, Andersen JL, Ardon O, DeHart JL, Blackett J *et al.* (2004). *Mol Cell Biol* **24**: 9286–9294.

Supplementary Information accompanies the paper on the Oncogene website (http://www.nature.com/onc).

HIV-1 Vpr Induces DNA Double-Strand Breaks

Hiroaki Tachiwana,[1,2] Mari Shimura,[2] Chikako Nakai-Murakami,[2] Kenzo Tokunaga,[3] Yoshimasa Takizawa,[1,2] Tetsutaro Sata,[3] Hitoshi Kurumizaka,[1] and Yukihito Ishizaka[2]

[1]Graduate School of Science and Engineering, Waseda University; [2]Department of Intractable Diseases, International Medical Center of Japan; and [3]Department of Pathology, National Institute of Infectious Diseases, Tokyo, Japan

Abstract

Recent observations imply that HIV-1 infection induces chromosomal DNA damage responses. However, the precise molecular mechanism and biological relevance are not fully understood. Here, we report that HIV-1 infection causes double-strand breaks in chromosomal DNA. We further found that Vpr, an accessory gene product of HIV-1, is a major factor responsible for HIV-1–induced double-strand breaks. The purified Vpr protein promotes double-strand breaks when incubated with isolated nuclei, although it does not exhibit endonuclease activity *in vitro*. A carboxyl-terminally truncated Vpr mutant that is defective in DNA-binding activity is less capable of Vpr-dependent double-strand break formation in isolated nuclei. The data suggest that double-strand breaks induced by Vpr depend on its DNA-binding activity and that Vpr may recruit unknown nuclear factor(s) with positive endonuclease activity to chromosomal DNA. This is the first direct evidence that Vpr induces double-strand breaks in HIV-1–infected cells. We discuss the possible roles of Vpr-induced DNA damage in HIV-1 infection and the involvement of Vpr in further acquired immunodeficiency syndrome–related tumor development. (Cancer Res 2006; 66(2): 627-31)

Introduction

A high incidence of malignant tumors, such as non-Hodgkin's lymphoma, Kaposi's sarcoma, and invasive cervical cancer [acquired immunodeficiency syndrome (AIDS)–defining cancers], is epidemiologically associated with HIV-1 infection (1, 2). These neoplasms are attributable mainly to diseases that accompany immunodeficiency, including coinfection with EBV, human herpes virus 8, and human papillomavirus (1, 2). In addition to these AIDS-defining cancers, several non-AIDS-defining cancers also occur with a higher incidence in HIV-infected individuals (3, 4). These reports lead to the assumption that HIV-1 has the potential to induce neoplasms before AIDS develops. Recently, DNA damage responses have been observed in precancerous lesion before inactivation of p53 (5, 6). Interestingly, it has been reported that HIV-1 infection induces DNA damage responses by activating Rad3-related or ataxia-telangiectasia mutated proteins and promoting phosphorylation of their downstream substrates (7, 8). The elucidation of the factor triggering the DNA damage responses to HIV-1 infection is essential to determine the as yet unknown mechanism causing AIDS-related neoplasms. In the present study, we found that HIV-1 infection induces double-strand breaks of chromosomal DNA, as detected using pulsed-field gel electrophoresis (PFGE). We further showed that *vpr*, an accessory gene of HIV-1 encoding a virion-associated nuclear protein, which induces cell cycle accumulation at G_2-M phase and increases ploidy (9), was a factor responsible for double-strand breaks. We discuss the potential ability of Vpr-induced double-strand breaks to develop into neoplasms in HIV-1 infection.

Materials and Methods

Cell culture. MIT-23 and ΔVpr, a mock transfectant, were established from HT1080 (JCRB9113; the Health Science Research Resources Bank) as previously described (9). In MIT-23, Vpr expression is controlled by the rtet promoter on incubation with 3 μg/mL doxycycline (Sigma, St. Louis, MO) for 48 hours.

Virus infection. Vesicular stomatitis virus G protein (VSV-G)–pseudotyped HIV-1 was produced by cotransfection with a plasmid encoding VSV-G (pHIT/G) and the pNL-Luc-E$^-$R$^+$ or pNL-Luc-E$^-$R$^-$ proviral clone (10). (10). The preparation and titration of viruses are described elsewhere (11). Briefly, the concentration of p24 antigen in the culture supernatant was measured using a p24 Gag antigen capture ELISA kit (ZeptoMetrix, Buffalo, NY). The infectivity of the prepared viral stock was examined using MAGIC5 cells. HT1080 cells were infected for 48 hours with viruses that had 200 ng/mL of p24 Gag antigen, giving a multiplicity of infection (MOI) of 0.7.

Immunostaining. Immunostaining was carried out as described (9). A rabbit polyclonal Rad51 antibody raised against the bacterially expressed protein and a mouse monoclonal antibody raised against synthesized peptides of full-length of Vpr (mAb8D1) were used as the primary antibody. Goat anti-rabbit IgG conjugated with Alexa Fluor 488 (Molecular Probes, Inc., Eugene, OR) and goat anti-mouse IgG conjugated with Cy3 (Zymed Laboratories, Inc., San Francisco, CA) were used as the secondary antibodies. Images were captured on a phase contrast microscope, BX50 (Olympus Corp., Tokyo Japan), or a Radiance 2100 laser scanning confocal microscope (Carl Zeiss, Oberkochen, Germany).

Overexpression and purification of Vpr and its mutant. The HIV-1 *vpr* gene was ligated into the *Nde*I and *Bam*HI sites of the pET15b vector (Novagen, Madison, WI). The Vpr protein and VprΔC12 mutant were produced in the *Escherichia coli* BL21 (DE3) Codon(+)RIL strain (Novagen) by induction with isopropyl-β-D-thiogalactopyranoside (IPTG; Nacalai Tesque, Inc., Kyoto, Japan) and were purified as described in Supplementary Method. The concentration of the purified Vpr protein was determined with a Bio-Rad protein assay kit (Bio-Rad Laboratories, Hercules, CA) using bovine serum albumin (BSA) as the standard.

Isolation of nuclei. Cells scraped from culture dishes were washed once with ice-cold PBS and resuspended in 3 mL of ice-cold 20 mmol/L Tris-HCl buffer (pH 7.6) containing 60 mmol/L KCl, 15 mmol/L NaCl, 5 mmol/L $MgCl_2$, 1 mmol/L DTT, 250 mmol/L sucrose, 0.6% NP40, and

Note: Supplementary data for this article are available at Cancer Research Online (http://cancerres.aacrjournals.org/).

Requests for reprints: Hitoshi Kurumizaka, Graduate School of Science and Engineering, Waseda University, 3-4-1 Okubo, Shinjuku-ku, 169-8555 Tokyo, Japan. Phone: 81-3-5286-8189; Fax: 81-3-5292-9211; E-mail: kurumizaka@waseda.jp and Yukihito Ishizaka, Department of Intractable Diseases, International Medical Center of Japan, 1-21-1 Toyama, Shinjuku-ku, 162-8655 Tokyo, Japan. Phone: 81-3-5272-7527; E-mail: zakay@ri.imcj.go.jp.

doi:10.1158/0008-5472.CAN-05-3144

protease inhibitor mixture (Sigma). The cell suspension was incubated for 10 minutes on ice and the sucrose concentration was adjusted to 1.6 mol/L. Then, the sample was loaded onto a sucrose cushion of 2.3 mol/L sucrose solution and centrifuged at 35,000 × *g* for 30 minutes. The isolated nuclei were obtained in the 2.3 mol/L sucrose fraction. For immunostaining, isolated nuclei were cytocentrifuged to the MAS-coated slide glass (Matsunami Glass IND., LTD., Tokyo, Japan) for 6 minutes at 800 rpm (Thermo Shandon, Chadwick Road, United Kingdom).

PFGE assay. Isolated nuclei were incubated with 10 μmol/L of purified Vpr or VprΔC12 for 15 hours at 30°C. The cells (isolated nuclei) were embedded in agarose plugs at a density of 3 × 10^5 cells/100 μL. The plugs were treated with proteinase K solution [0.5 mol/L EDTA (pH 8.0), 1% sarcosyl, and 0.5 mg/mL proteinase K] for 38 hours at 50°C. After PFGE was done in a CHEFF Mapper (Bio-Rad Laboratories), the gels were stained with Vistra Green (Amersham Bioscience, Piscataway, NJ).

The DNA-binding assay. The Vpr protein was incubated with ϕX174 single-stranded DNA (ssDNA; 20 μmol/L) or ϕX174 superhelical dsDNA (10 μmol/L) in 10 μL of 8 mmol/L Tris-HCl buffer (pH 8.5) containing 1 mmol/L DTT and 100 μg/mL BSA. The reaction mixtures were incubated for 1 hour at 37°C and were analyzed by electrophoresis on a 0.8% agarose gel in 1× TAE buffer (40 mmol/L Tris acetate and 1 mmol/L EDTA) at 3.3 V/cm for 2 hours. The bands were visualized using ethidium bromide staining.

Nuclease activity. The Vpr protein (18.8 μmol/L) or DNaseI (Invitrogen Corporation, Carlsbad, CA; 0.02 unit/μL) were incubated with ϕX174 superhelical double-stranded DNA (dsDNA; 2.5 μmol/L) in 40 μL of 15 mmol/L Tris-HCl buffer (pH 8.5) containing 1 mmol/L DTT and 100 μg/mL BSA, in the presence of 5 mmol/L $MgCl_2$, $MnCl_2$, $ZnSO_4$, or $CaCl_2$. The reaction mixtures were incubated at 37°C for 30 minutes. After incubation, the samples were treated with proteinase K (0.3 mg/mL) in the presence of 0.1% SDS and the DNA was extracted using phenol-chloroform. The DNA was precipitated by ethanol and was analyzed by electrophoresis on a 0.8% agarose gel in 1 × TAE buffer at 6.6 V/cm for 30 minutes. The bands were visualized with ethidium bromide staining.

The Ni-NTA agarose pull-down assay. Isolated nuclei were disrupted in 20 mmol/L Tris-HCl buffer (pH 8.5) containing 200 mmol/L KCl, 2 mmol/L 2-mercaptoethanol, 0.25 mmol/L EDTA, and 10% glycerol. The extract was incubated with His_6-Vpr (53 μmol/L) for 15 hours at 30°C. After incubation, His_6-Vpr was precipitated with 4 μL of Ni-NTA agarose beads and the beads were washed thrice with 500 μL of 20 mmol/L Tris-HCl buffer (pH 7.6) containing 100 mmol/L NaCl, 5 mmol/L DTT, 10 mmol/L imidazole, 1 mmol/L EDTA, and 0.2% Tween 20. The proteins precipitated with the Ni-NTA beads were analyzed by 16% SDS-PAGE. The bands were visualized by silver staining.

Results

Vpr expression induces chromosomal double-strand breaks. To test whether HIV-1 infection causes double-strand breaks, we used PFGE, which was able to clearly detect the double-strand breaks induced by X-ray irradiation (Fig. 1*A*, *lane 2*; ref. 12). HT1080 cells were infected with HIV-1 that had 200 ng/mL of p24 Gag antigen, giving a MOI of 0.7, and the cellular DNA was fractionated using PFGE. Figure 1*A* (*lane 6*) shows that HIV-1 infection induced double-strand breaks. Interestingly, the amount of HIV-1-dependent double-strand breaks was reduced significantly (Fig. 1*A*, *lane 5*) when the *vpr* gene was deleted from the HIV-1 viral genome (HIV-1ΔVpr). To show that HIV-1-dependent double-strand breaks are attributable to Vpr expression, we examined double-strand break formation in Vpr stable transfectant, MIT-23 (9), in which Vpr expression is controlled by the rtet promoter by doxycycline, and, in ΔVpr, a mock transfectant. As shown in Fig. 1*B*, double-strand breaks were observed in the Vpr-expressing cells (*lane 5, arrow*) but not in the mock transfectants (*lane 4*). Furthermore, Rad51 foci, which are formed

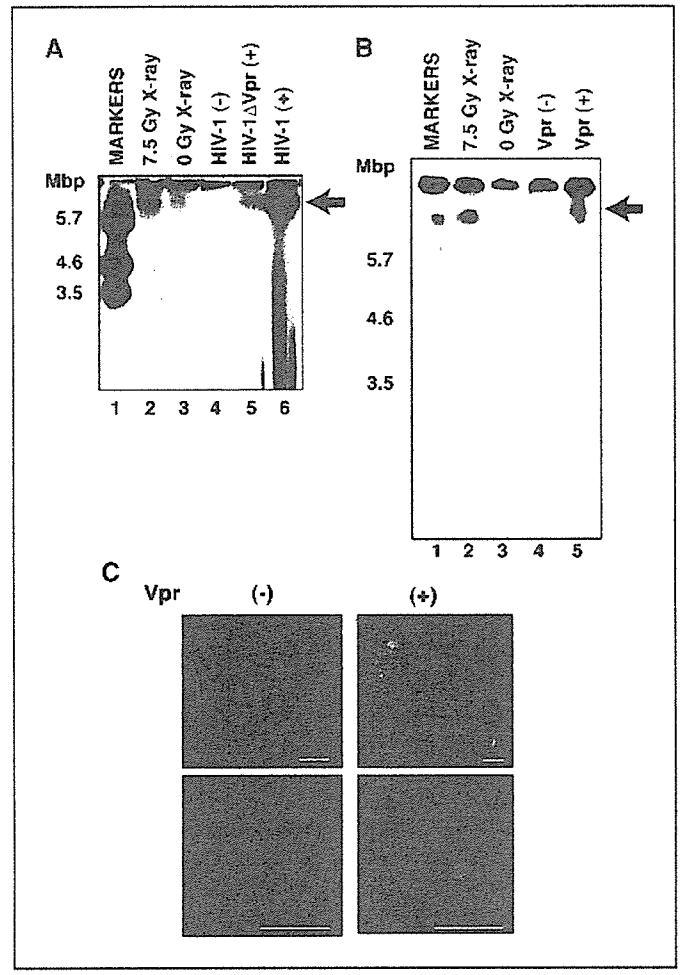

Figure 1. Vpr induces double-strand breaks *in vivo*. *A*, PFGE analysis of double-strand breaks after HIV-1 infection. HT1080 cells were infected with the same amount of HIV-1 or HIV-1ΔVpr (MOI = 0.7) and subjected to PFGE. As a positive control, uninfected cells were analyzed immediately after 7.5 Gy of X-ray irradiation. Molecular mass markers (*lane 1*), control cells (*lanes 3* and *4*), cells subjected to X-ray irradiation (*lane 2*), and cells infected with HIV-1ΔVpr (*lane 5*) or HIV-1 (*lane 6*) are shown. *Arrow*, position corresponding to the double-strand breaks. *B*, PFGE analysis in Vpr-expressing cells. Molecular mass markers (*lane 1*), cells irradiated with 7.5 Gy (*lane 2*), control cells (*lane 3*), mock transfectants (*lane 4*), and cells with Vpr expression (*lane 5*) are shown. *Arrow*, double-strand breaks. *C*, Rad51 focus formation with Vpr expression. An immunohistochemical analysis was used to detect Rad51 in cells with (*right*) or without (*left*) Vpr expression. Bar, 10 μm.

at double-strand break sites (13), were observed with Vpr expression (Fig. 1*C*). These results indicate that Vpr is responsible for double-strand break formation. The double-strand breaks shown in Fig. 1*B* were not the result of an apoptotic process as the DNA ladder typically observed in apoptotic cells (14) was not detected (data not shown).

Vpr has no endonuclease activity. Next, we studied whether Vpr directly induces double-strand breaks. The recombinant Vpr protein was purified to near homogeneity (Fig. 2*A*) and the DNA-binding activity of Vpr was examined. As shown in Fig. 2*B*, purified Vpr bound both ssDNA (*lanes 2-6*) and dsDNA (*lanes 8-12*) in an ATP- and Mg^{2+}-independent manner (15). Then, we examined whether Vpr has nuclease activity. Superhelical dsDNA containing small amounts of nicked circular dsDNA was incubated with Vpr in the presence of various divalent cations. After the incubation, the proteins were removed and the DNA was examined by

electrophoresis. If Vpr induces a double-strand break or nick, the superhelical dsDNA would give rise to linear or nicked circular forms, producing a different electrophoretic pattern. However, the DNA incubated with Vpr in the absence (*lane 2*) or presence of any divalent cation examined (*lanes 4, 6, 8,* and *10*) showed the same migration pattern with control (*lane 1*), indicating that Vpr does not cleave DNA (Fig. 2*C*). Positive control experiments showed that the DNA was digested by DNaseI with $MgCl_2$, $MnCl_2$, or $CaCl_2$ (*lanes 5, 7,* and *11*) but not with $ZnSO_4$ (*lane 9*; Fig. 2*C*). Therefore, these results indicate that Vpr lacks endonuclease or nicking activity.

Vpr induces double-strand breaks *in vitro*. In a second approach, we tested whether purified Vpr induces double-strand breaks in nuclei isolated from HT1080 cells (Fig. 3*A*). First, we confirmed by a laser confocal microscopy that Vpr localizes in nuclei after incubation *in vitro* (Fig. 3*B*). The nuclear DNA was then analyzed for double-strand breaks by using PFGE (Fig. 3*C*). Interestingly, purified Vpr induced double-strand breaks in the DNA of the isolated nuclei (Fig. 3*C, lane 5, arrow*). By contrast, few double-strand breaks were detected without Vpr (Fig. 3*C, lane 4*). Because Vpr alone did not show endonuclease activity (Fig. 2*C*), these results suggest that Vpr interacts with intrinsic nuclear protein(s), which required for double-strand break formation. To identify candidates for the Vpr-interacting nuclear proteins, we did the Ni-NTA pull-down assay. In this assay, recombinant His_6-tagged Vpr was incubated with the extract from isolated nuclei and Ni-NTA beads precipitated proteins bound to His_6-tagged Vpr (Fig. 3*D*). As shown in Fig. 3*D*, His_6-tagged Vpr associated with numerous proteins that were not detected in the control precipitates (*lane 2, asterisks*).

The DNA-binding activity of Vpr is correlated with double-strand break formation. The COOH-terminal region of Vpr is arginine rich and is thought to be an important site for DNA binding to Vpr (15). Nuclear magnetic resonance analysis shows that Vpr has three α-helixes (amino acids 17-33, 38-50, and 56-77) in solution, whereas the COOH-terminal region from amino acid residues 84 to 96 is disordered (16). This suggests that the deletion of the COOH-terminal 12 amino acid residues does not affect the tertiary structure of Vpr. We purified a Vpr mutant protein lacking the COOH-terminal 12-amino-acid residues (VprΔC12; Fig. 4*A*), and examined its DNA-binding activity. Purified VprΔC12 was significantly defective in both ssDNA- and dsDNA-binding activity compared with wild-type Vpr (Fig. 4*B*). Interestingly, VprΔC12 induced double-strand breaks in isolated nuclei but its efficiency was reduced significantly (Fig. 4*C, lane 6*). These results indicate that the DNA-binding ability of Vpr is important for the induction of double-strand breaks by Vpr.

Discussion

Here, we present evidence that HIV-1 Vpr induces double-strand breaks. Our data are consistent with previous observations in Vpr-expressing cells: the up-regulation of gene amplification events that are believed to be introduced by broken DNA strands (17) and the activation of activating Rad3-related/ataxia-telangiectasia mutated, followed by the phosphorylation of their downstream substrate, a histone H2A variant, H2AX, and γ-H2AX and BRCA1 focus formation (8). Biochemical analyses using purified Vpr indicated that Vpr alone has no endonuclease activity (Fig. 2*C*), suggesting that a cellular factor(s), possibly with endonuclease activity, is required for Vpr-dependent double-strand breaks. The factor(s) required for double-strand breaks must preexist in nuclei because double-strand breaks were observed upon incubating a mixture of isolated nuclei and purified Vpr *in vitro* (Fig. 3*C*). As one possible mechanism, Vpr may recruit a nuclease factor to chromosomal DNA, given that the Vpr-dependent double-strand breaks were correlated with the DNA-binding activity (Figs. 4*B* and *C*). Alternatively, Vpr itself may acquire endonuclease activity after modification in the nucleus. Further analyses are necessary to clarify this point.

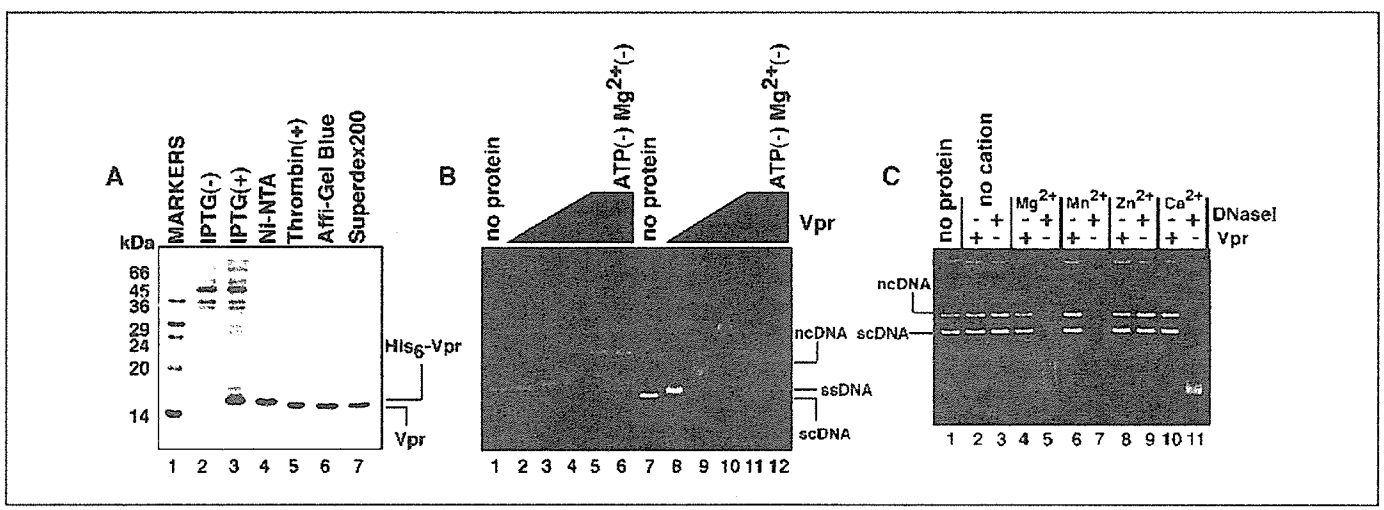

Figure 2. The Vpr-DNA interaction *in vitro*. *A*, purification of recombinant Vpr. Proteins from each purification step were analyzed using 16% SDS-PAGE with Coomassie brilliant blue staining. Molecular mass markers (*lane 1*), whole-cell lysates before (*lane 2*) and after (*lane 3*) induction with IPTG, samples from the Ni-NTA fraction (*lane 4*), the fraction after removing the hexahistidine tag (*lane 5*), the Affi-Gel Blue fraction (*lane 6*), and the Superdex 200 fraction (*lane 7*) are shown. *B*, the DNA-binding activity of Vpr. ϕX174 circular ssDNA (20 μmol/L; *lanes 2-6*) and ϕX174 superhelical dsDNA (*scDNA*; 10 μmol/L; *lanes 8-12*) containing a small amount of nicked circular DNA (*ncDNA*) were incubated with Vpr in the presence of 1 mmol/L ATP and 1 mmol/L $MgCl_2$. Control experiments without ATP and $MgCl_2$ (*lanes 6* and *12*) are included. The Vpr concentrations were 1.25 μmol/L (*lanes 2* and *8*), 2.5 μmol/L (*lanes 3* and *9*), 5 μmol/L (*lanes 4* and *10*), and 10 μmol/L (*lanes 5, 6, 11,* and *12*). *Lanes 1* and *7*, negative controls without protein. *C*, nuclease activity. ϕX174 scDNA (2.5 μmol/L) was incubated with Vpr (18.8 μmol/L; *lanes 2, 4, 6, 8,* and *10*) or DNaseI (*lanes 3, 5, 7, 9,* and *11*) in the absence of divalent cation (*lanes 2* and *3*) or in the presence of 5 mmol/L $MgCl_2$ (*lanes 4* and *5*), 5 mmol/L $MnCl_2$ (*lanes 6* and *7*), 5 mmol/L $ZnSO_4$ (*lanes 8* and *9*), or 5 mmol/L $CaCl_2$ (*lanes 10* and *11*). *Lane 1*, negative control without protein.

In the HIV-1 life cycle, DNA breakage and repair are thought to be essential steps for integrating the double-stranded viral cDNA into the host genome. In this study, we found that Vpr is one molecule responsible for the double-strand breaks that occur upon HIV-1 infection. However, it is also noteworthy that some double-strand breaks were induced in the cells with HIV-1ΔVpr (Fig. 1*A*, *lane 5*), suggesting that other viral factors are also involved. It has been shown that integrase activates the ataxia-telangiectasia mutated–dependent pathway (7) and, thus, the double-strand breaks observed with HIV-1ΔVpr infection are probably owing to integrase. For viral integration to occur, the amount of double-strand breaks induced by HIV-1ΔVpr (Fig. 1*A*, *lane 5*) may be sufficient, because viral production in peripheral blood mononuclear cells was not alleviated by infection with

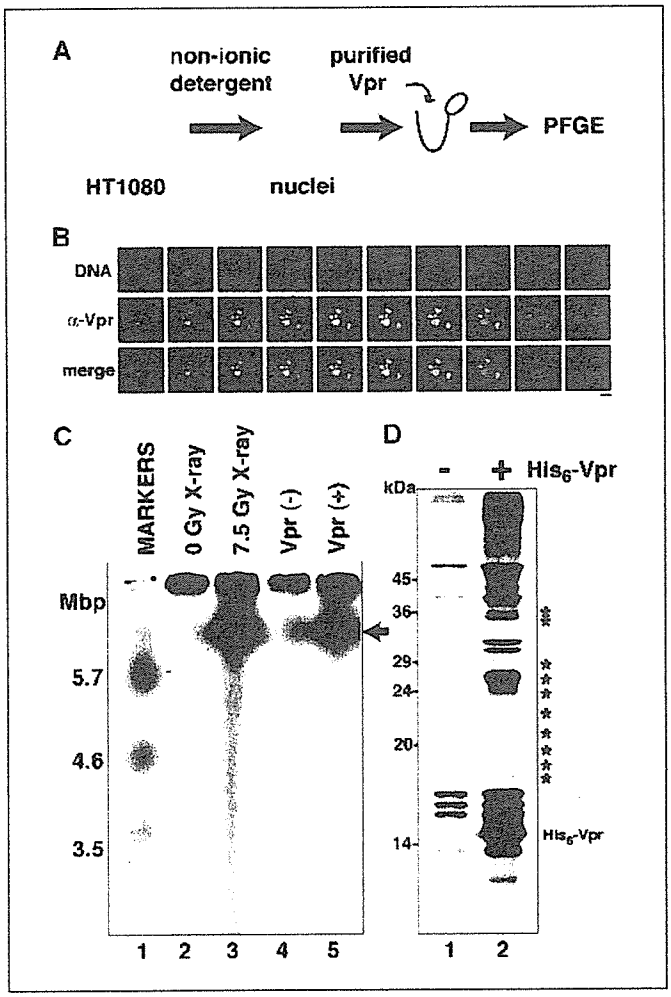

Figure 3. Purified Vpr induces double-strand breaks *in vitro*. *A*, a scheme of the protocol used to detect Vpr-induced double-strand breaks in isolated nuclei. *B*, Vpr localization in isolated nuclei. Isolated nuclei from HT1080 after incubation with Vpr were immunostained by α-Vpr (mAb8D1) and the images were captured by a laser confocal microscopy. The Z-series of optical sections collected at 1 μm steps of the cells were presented. Vpr (*red; middle*), DNA staining by Hoechst (*blue; top*) and their merged images (*bottom*) are shown. Without Vpr incubation, any signals by α-Vpr immunostaining were not detected in isolated nuclei (data not shown). Bar, 10 μm. *C*, PFGE analysis of double-strand breaks in isolated nuclei treated with Vpr. Molecular mass markers (*lane 1*), control cells (*lane 2*), cells subjected to X-ray irradiation (*lane 3*), and isolated nuclei without (*lane 4*) or with 10 μmol/L Vpr (*lane 5*). *Arrow*, double-strand breaks. *D*, Ni-NTA pull-down assay with His_6-tagged Vpr on isolated nuclei. Precipitated proteins bound to His_6-tagged Vpr (*lane 2*) and the control precipitates (*lane 1*) are indicated. *, His_6-Vpr–specific bands.

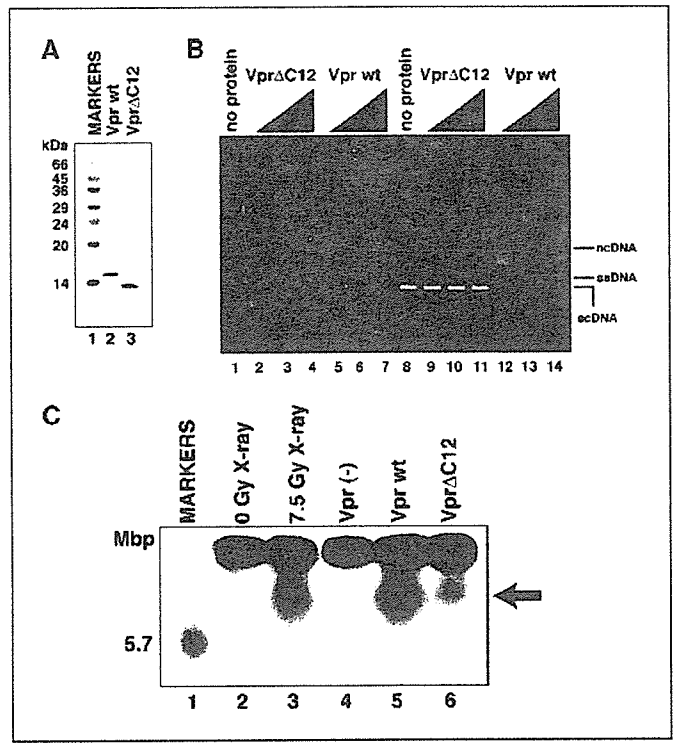

Figure 4. DNA-binding and double-strand break formation by Vpr. *A*, purification of VprΔC12. Purified VprΔC12 was analyzed using 16% SDS-PAGE with Coomassie brilliant blue staining. *Lane 1*, molecular mass markers. *Lanes 2* and *3*, purified wild-type Vpr and VprΔC12 protein, respectively. *B*, the DNA-binding activity of VprΔC12. The DNA-binding experiments were done using the protocol used to obtain Fig. 2*B*. The concentrations of VprΔC12 were 2.5 μmol/L (*lanes 2* and *9*), 5 μmol/L (*lanes 3* and *10*), and 10 μmol/L (*lanes 4* and *11*), and those of the wild-type Vpr were 2.5 μmol/L (*lanes 5* and *12*), 5 μmol/L (*lanes 6* and *13*), and 10 μmol/L (*lanes 7* and *14*). Negative controls without protein (*lanes 1* and *8*) are included. *C*, PFGE analysis of double-strand breaks in isolated nuclei treated with Vpr or VprΔC12. Molecular mass marker (*lane 1*), cells without (*lane 2*) or with (*lane 3*) 7.5 Gy of X-ray irradiation, control nuclei (*lane 4*), nuclei with Vpr (*lane 5*), and nuclei with VprΔC12 (*lane 6*). Vpr was used at 10 μmol/L. *Arrow*, double-strand breaks.

Vpr-deleted HIV-1 (18).[4] Vpr-induced double-strand breaks may be surplus to those required for viral integration (Fig. 1*A*, *lane 6*). The resultant DNA damage may reduce the integrity of the host genome.

Recently, DNA damage signaling was observed at an early stage of tumor development, suggesting that the DNA damage response is a mechanism to prevent the progression of pre-neoplasic lesions (5). If DNA repair is not accomplished correctly or is skipped because of unregulated checkpoint controls, the genomic structure would be altered severely (19). The progression of malignant tumors in AIDS-defining cancers is well documented in oncovirus infections (1, 2). If DNA damage increases the probability of neoplasia, Vpr-induced double-strand breaks with oncovirus infection may accelerate tumor progression during the clinical course of AIDS. In addition to AIDS-defining cancers, non-AIDS-defining cancers also occur at a higher incidence and the factor responsible for such oncogenesis is now a critical issue (3, 4). Vpr-induced DNA damage may result in

[4] M. Shimura, unpublished data.

these AIDS-related malignancies. It is essential to explore the molecular mechanism of Vpr-induced double-strand breaks to clarify their role in HIV-1 infection and their effect on the stability of the host cell genome.

Acknowledgments

Received 9/1/2005; revised 11/16/2005; accepted 11/22/2005.

Grant support: Grants-in-Aid for Scientific Research from the Ministry of Health, Labor, and Welfare of Japan; the Japanese Society for the Promotion of Science; the Ministry of Education, Sports, Culture, Science, and Technology of Japan; and a research grant from the Kato Memorial Trust for Nambyo Research and the Japan Health Sciences Foundation.

The costs of publication of this article were defrayed in part by the payment of page charges. This article must therefore be hereby marked *advertisement* in accordance with 18 U.S.C. Section 1734 solely to indicate this fact.

We thank Dr. Masashi Tatsumi (National Institute of Infectious Diseases, Tokyo, Japan) for providing us with MAGIC5 cells and Koji Nakatani for his technical assistance and heart-warming support.

References

1. Beral V, Peterman T, Berkelman R, Jaffe H. AIDS-associated non-Hodgkin lymphoma. Lancet 1991;337:805–9.
2. Bellan C, De Falco G, Lazzi S, Leoncini L. Pathologic aspects of AIDS malignancies. Oncogene 2003;22:6639–45.
3. Wistuba II, Behrens C, Gazdar AF. Pathogenesis of non-AIDS-defining cancers: a review. AIDS Patient Care STDS 1999;13:415–26.
4. Chiao EY, Krown SE. Update on non-acquired immunodeficiency syndrome-defining malignancies. Curr Opin Oncol 2003;15:389–97.
5. Bartkova J, Horejsi Z, Koed K, et al. DNA damage response as a candidate anti-cancer barrier in early human tumorigenesis. Nature 2005;434:864–70.
6. Gorgoulis VG, Vassiliou L-VF, Karakaidos P, et al. Activation of the DNA damage checkpoint and genomic instability in human precancerous lesions. Narture 2005;434:907–13.
7. Lau A, Swinbank KM, Ahmed PS, et al. Suppression of HIV-1 infection by a small molecule inhibitor of the ATM kinase. Nat Cell Biol 2005;7:493–500.
8. Zimmerman ES, Chen J, Andersen JL, et al. Human immunodeficiency virus type 1 Vpr-mediated G_2 arrest requires Rad17 and Hus1 and induces nuclear BRCA1 and γ-H2AX focus formation. Mol Cell Biol 2004;24:9286–94.
9. Shimura M, Tanaka Y, Nakamura S, et al. Micronuclei formation and aneuploidy induced by Vpr, an accessory gene of human immunodeficiency virus type 1. FASEB J 1999;13:621–37.
10. Adachi A, Gendelman HE, Koenig S, et al. Production of acquired immunodeficiency syndrome-associated retrovirus in human and nonhuman cells transfected with an infectious molecular clone. J Virol 1986;59:284–91.
11. Tokunaga K, Greenberg ML, Morse MA, Cumming RI, Lyerly HK, Cullen BR. Molecular basis for cell tropism of CXCR4-dependent human immunodeficiency virus type 1 isolates. J Virol 2001;75:6776–85.
12. Krüger I, Rothkamm K, Löbrich M. Enhanced fidelity for rejoining radiation-induced DNA double-strand breaks in the G_2 phase of Chinese hamster ovary cells. Nucleic Acids Res 2004;32:2677–84.
13. Haaf T, Golub EI, Reddy G, Radding CM, Ward DC. Nuclear foci of mammalian Rad51 recombination protein in somatic cells after DNA damage and its localization in synaptonemal complexes. Proc Natl Acad Sci U S A 1995;92:2298–302.
14. Maecker HT, Hedjbeli S, Alzona M, Le PT. Comparison of apoptosis signaling through T cell receptor, fas, and calcium ionophore. Exp Cell Res 1996;222:95–102.
15. Zhang S, Pointer D, Singer G, Feng Y, Park K, Zhao LJ. Direct binding to nucleic acids by Vpr of human immunodeficiency virus type 1. Gene 1998;212:157–66.
16. Morellet N, Bouaziz S, Petitjean P, Roques BP. NMR structure of the HIV-1 regulatory protein VPR. J Mol Biol 2003;327:215–27.
17. Shimura M, Onozuka Y, Yamaguchi T, Hatake K, Takaku F, Ishizaka Y. Micronuclei formation with chromosome breaks and gene amplification caused by Vpr, an accessory gene of human immunodeficiency virus. Cancer Res 1999;59:2259–64.
18. Kawano Y, Tanaka Y, Misawa N, et al. Mutational analysis of human immunodeficiency virus type 1 (HIV-1) accessory genes: requirement of a site in the nef gene for HIV-1 replication in activated $CD4^+$ T cells *in vitro* and *in vivo*. J Virol 1997;71:8456–66.
19. Furuta S, Jiang X, Gu B, Cheng E, Chen PL, Lee WH. Depletion of BRCA1 impairs differentiation but enhances proliferation of mammary epithelial cells. Proc Natl Acad Sci U S A 2005;102:9176–81.

Thermosensitive Polymers

DOI: 10.1002/anie.200603346

Comparison of Thermosensitive Properties of Poly(amidoamine) Dendrimers with Peripheral *N*-Isopropylamide Groups and Linear Polymers with the Same Groups

*Yasuhiro Haba, Chie Kojima, Atsushi Harada, and Kenji Kono**

Thermosensitive polymers, which exhibit changes in water solubility at a specific temperature, are highly attractive for the production of functional or intelligent materials.[1] Although a number of polymers are known to exhibit thermosensitive properties, the most thoroughly studied is poly(*N*-isopropylacrylamide) (PNIPAAm).[2,3] This polymer is highly soluble in water at low temperature. It becomes water-insoluble at temperatures greater than 31–32 °C: the polymer chains become dehydrated and form aggregates.[3] This temperature is designated as the lower critical solution temperature (LCST).

The thermosensitive polymers known so far generally possess a linear structure. However, recently we developed a new type of thermosensitive polymer with a globular structure. These polymers were obtained by modification of the chain terminals of poly(amidoamine) (PAMAM) or poly(propyleneimine) dendrimers with isobutyramide groups, which are common structural units in the thermosensitive polymer, poly(*N*-vinylisobutyramide).[4] These modified dendrimers differ markedly from conventional thermosensitive polymers with a linear structure in terms of their molecular shape and location of alkyl amide groups, which play a crucial role in determining their thermosensitive properties.

A number of studies comparing dendritic, hyperbranched, and linear polymers have revealed that molecular shapes and topologies strongly influence their chemical and physical properties.[5] In addition, the unique shape and characteristics of thermosensitive dendrimers may lead to the production of novel functional materials that are not obtainable with linear thermosensitive polymers. Therefore, we seek to elucidate how such differences affect their thermosensitive properties, which may lead to the generation of new applications for thermosensitive polymers.

In this study, we introduce the *N*-isopropylamide (NIPAM) group, which is a common structural unit with PNIPAAm, at every chain terminal of the PAMAM dendrimer through various spacers. The thermosensitive properties of the NIPAM-terminated dendrimers were compared with those of NIPAM-bearing polymers with a linear structure, such as PNIPAAm and poly(*N*-isopropylacrylamide-*co*-acrylamide) [poly(NIPAAm-*co*-AAm)].

The PAMAM dendrimers with NIPAM, *N*-isopropylsuccinamide, and 4-isopropylcarbamoyl butyramide groups at every chain end, which are designated as NIPAM-0-G4.5, NIPAM-3-G5, and NIPAM-4-G5, respectively, were synthesized by reacting a corresponding amine or carboxylic acid with the carboxyl-terminated PAMAM G4.5 or amine-terminated PAMAM G5 dendrimer, according to a previously reported method (Scheme 1).[4,6] Analysis by ^{1}H and ^{13}C NMR spectroscopy demonstrated that essentially every chain terminal of these dendrimers was connected to the corresponding terminal groups of the surface-modified dendrimers (see the Supporting Information).

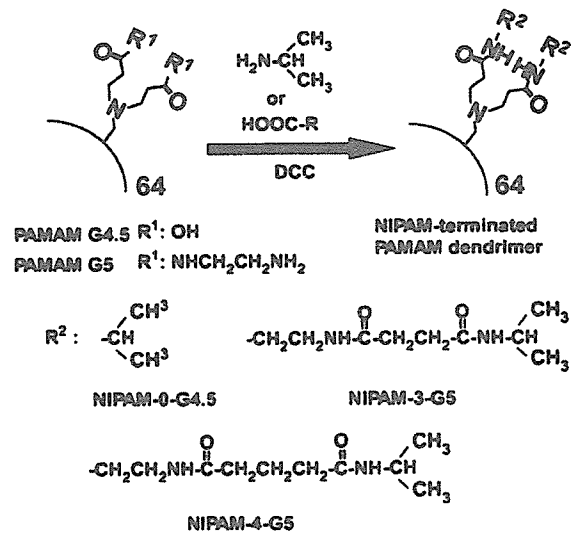

Scheme 1. Synthetic route for NIPAM-terminated dendrimers. DCC = 1,3-dicyclohexylcarbodiimide. The number 64 next to the gray surface refers to the humber of terminal moieties.

Figure 1 depicts the temperature dependence of the light transmittance of solutions of various NIPAM-terminated dendrimers and linear polymers with NIPAM groups in a phosphate solution (10 mM, pH 9.0) at 500 nm. PNIPAAm exhibited a sharp decrease in transmittance at 32 °C, which indicates that this polymer underwent conformational transition from a hydrated coil to a dehydrated globule at this temperature. Poly(NIPAAm-*co*-AAm) also showed a sharp decrease in transmittance at 40 °C.

[*] Y. Haba, Dr. C. Kojima, Dr. A. Harada, Prof. Dr. K. Kono
Department of Applied Chemistry
Osaka Prefecture University
1-1 Gakuen-cho, Nakaku, Sakai, Osaka 599-8531 (Japan)
Fax: (+81) 72-254-9330
E-mail: kono@chem.osakafu-u.ac.jp
Homepage: http://www.chem.osakafu-u.ac.jp/ohka/ohka9/engl.html

Supporting information for this article is available on the WWW under http://www.angewandte.org or from the author.